2DOF I-PD Model-Following Speed Controller for Field-Oriented Induction Motor Drive

FAYEZ F. M. EL-SOUSY
Power Electronics & Energy Conversion Department
Electronics Research Institute (ERI)
Al-Tahrir Street, Dokki, Giza, Egypt
EGYPT

Abstrat: - A robust controller that combines the merits of the feed-back, feed-forward and model following control for induction motor drive under field orientation control is designed in this paper. The proposed controller is a two-degrees-of-freedom (2DOF) integral plus proportional & rate feedback (I-PD) with model following (2DOF I-PD MFC) speed controller. A systematic mathimatical procedure is derived to find the parameters of the 2DOF I-PD MFC speed controller according to certain specifications for the drive system. Initially, we start with the I-PD feed-back controller design, then the feed-forward controller. These two controllers combine the 2DOF I-PD speed controller. To realize high dynamic performance for disturbance rejection and set point tracking characterisitics, a MFC controller is designed in addition to the 2DOF I-PD controller. This combination is called a 2DOF I-PD MFC speed controller. The dynamic performance of the drive system for different operating conditions is studied utilizing the 2DOF I-PD MFC speed controller. Computer simulation is carried out to demonstrate the effectiveness of the proposed controller. The results verify that the proposed 2DOF I-PD MFC controller can achieve accurate and robust performance for the drive system compared with the 2DOF I-PD speed controller in the presence of load disturbance and motor parameter variations. Also, the proposed controller grant a rapid and accurate response for the reference model, regardless of whether a load disturbance is imposed and the induction machine parameters vary.

Key-Words:: Indirect field orientation control, 2DOF I-PD controller, model following controllor (MFC), induction motor drive.

1 Introduction

Induction machines have many advantageous characteristics such as high robustness, reliability and low cost. Therefore, induction machine drives are used in high-performance industrial applications such as robotics, rolling mills, machine tools and tracking systems, which require independent torque and speed control. Induction machines also possess complex nonlinear, time-varying and tempereature dependency mathimatical model. The requirements of high dynamic performance is gained utilizing field orientation control (FOC) in which the dynamic model of the induction machine is simplified and decoupled. The FOC strategy is being studied in the context developed by Hass and Blashke in Germany some thirty years ago. This technique improves the performance of the induction machine drive system to a level comparable to that of the DC machine. Therefore, FOC of induction machine drive system has permitted high-performance dynamic response using the decoupled torque and flux control. In order to execute the indirect field orientation control (IFOC) strategy, current regulated pulse width modulated (CRPWM) inverters are usually employed to satisfy the current control requirements [1-4].

In many industrial drives, the control of field oriented induction machine drive with a conventional controllers have gained the widest acceptance in high-performance ac drive systems. However, the conventional controllers has difficulty in dealing with dynamic speed tracking, parameter variations and load disturbances. So, the dynamic performance of a field-oriented induction motor is affected by the decoupling characteristics. It is known that for the IFOC of induction motor drive, the ideal decoupling between the flux and torque will not be obtained if the rotor parameters used in the FOC can not track their nominal values. The most important parameter to be considered is the rotor resistance. The adaptation of FOC equation, ω_{sl}, is very important to achieve ideal decoupling. To reduce the effects of rotor parameter variations on IFOC, various tuning techniques have been reported [5-8]. There are several control

techniques for induction motor drive system to yield high–performance. One of the most commonly used controllers in industrial applications is the proportional plus integral plus derivative (PID) controller. Also, a modified structures of the PID controller such as PI-D and I-PD controllers are reported but these controllers achieved the tracking and regulation characteristics owing to the one-degree-of-freedom structure. A two-degrees-of-freedom (2DOF) IP or PI-D controllers has been designed for tracking and regulation performance characteristics for the induction machine in the previous work [9-14].

The author propose a hybrid controller, which combines the advantages of the two-degrees-of-freedom (2DOF) and the model following control techniques for the speed control of the induction motor drive. This IFOC induction motor drive system is composed of non-linear and linearzed dynamic models of the induction motor in the general reference frame, the dynamic model of the IFOC technique (decoupling controller), *d-q* axes stator current controllers, speed controller, space vector PWM modulator and PWM inverter.

This paper presents quantitative analysis and design of the 2DOF I-PD MFC speed controller for field oriented induction motor drive system. The controller is designed to achieve zero steady state error, minimum overshoot and minimum settling time, (good dynamic response for disturbance rejection and set point tracking). The proposed 2DOF I-PD controller consists of a I-PD type in the feed-back loop (also called integral plus proportional & rate feedback) and a feedd-forward controller. To realize high dynamic performance for disturbance rejection and set point tracking characteristics, a model following controller (MFC) is designed and analyzed in addition to the 2DOF I-PD speed controller. A quantitative design procedure is derived to find the parameters of the controller systematically according to the given motor specifications. In addition to the tracking and regulation speed control specifications, the effect of command change rate as well as control effort are also considered in the proposed design procedure. To verify the design of controller and system performance, the drive system is simulated. Taking into consideration the parameter variations of the induction machine, the dynamic performance have been studied under load changes. The simulation results are provided to demonstrate the effectiveness of the proposed controllers.

2 Dynamic Model of Induction Motor

2.1 Non-Linear Dynamic Model

The state equation of the nonlinear dynamic *d-q* model of the induction machine at the synchronous reference frame is expressed as follows [4].

$$\frac{d}{dt}\begin{bmatrix} i_{qs} \\ i_{ds} \end{bmatrix} = \begin{bmatrix} -k_{ss} & -\omega \\ \omega & -k_{ss} \end{bmatrix}\begin{bmatrix} i_{qs} \\ i_{ds} \end{bmatrix} + \begin{bmatrix} \frac{k_m}{\tau_r} & -k_m\omega_r \\ k_m\omega_r & \frac{k_m}{\tau_r} \end{bmatrix}\begin{bmatrix} \lambda_{qr} \\ \lambda_{dr} \end{bmatrix} + \frac{1}{\sigma L_s}\begin{bmatrix} V_{qs} \\ V_{ds} \end{bmatrix} \quad (1)$$

$$\frac{d}{dt}\begin{bmatrix} \lambda_{qr} \\ \lambda_{dr} \end{bmatrix} = \begin{bmatrix} \frac{L_m}{\tau_r} & 0 \\ 0 & \frac{L_m}{\tau_r} \end{bmatrix}\begin{bmatrix} i_{qs} \\ i_{ds} \end{bmatrix} + \begin{bmatrix} -\frac{1}{\tau_r} & -(\omega - \omega_r) \\ (\omega - \omega_r) & -\frac{1}{\tau_r} \end{bmatrix}\begin{bmatrix} \lambda_{qr} \\ \lambda_{dr} \end{bmatrix} \quad (2)$$

$$\frac{d}{dt}\omega_r = -\frac{\beta}{J}\omega_r + \frac{(P/2)}{J}T_e - \frac{(P/2)}{J}T_L \quad (3)$$

$$T_e = \frac{3}{2}.\frac{P}{2}.\frac{L_m}{L_r}(\lambda_{dr} i_{qs} - \lambda_{qr} i_{ds}) \quad (4)$$

2.2 Linear Dynamic Model

For facilitating the analysis and design of the proposed controllers, the linear dynamic model for the induction machine is developed. From equations (1-4), we can derive the perturbed model of the induction machine as follows:

$$\frac{d}{dt}\begin{bmatrix} \Delta i_{qs} \\ \Delta i_{ds} \end{bmatrix} = \begin{bmatrix} -k_{ss} & -\omega_o \\ \omega_o & -k_{ss} \end{bmatrix}\begin{bmatrix} \Delta i_{qs} \\ \Delta i_{ds} \end{bmatrix} + \begin{bmatrix} \frac{k_m}{\tau_r} & -k_m\omega_{ro} \\ k_m\omega_{ro} & \frac{k_m}{\tau_r} \end{bmatrix}\begin{bmatrix} \Delta\lambda_{qr} \\ \Delta\lambda_{dr} \end{bmatrix} + \frac{1}{\sigma L_s}\begin{bmatrix} \Delta V_{qs} \\ \Delta V_{ds} \end{bmatrix} \quad (5)$$

$$\frac{d}{dt}\begin{bmatrix} \Delta\lambda_{qr} \\ \Delta\lambda_{dr} \end{bmatrix} = \begin{bmatrix} \frac{L_m}{\tau_r} & 0 \\ 0 & \frac{L_m}{\tau_r} \end{bmatrix}\begin{bmatrix} \Delta i_{qs} \\ \Delta i_{ds} \end{bmatrix} + \begin{bmatrix} -\frac{1}{\tau_r} & -(\omega_o - \omega_{ro}) \\ (\omega_o - \omega_{ro}) & -\frac{1}{\tau_r} \end{bmatrix}\begin{bmatrix} \Delta\lambda_{qr} \\ \Delta\lambda_{dr} \end{bmatrix} \quad (6)$$

$$\frac{d}{dt}\Delta\omega_r = -\frac{\beta}{J}\Delta\omega_r + \frac{(P/2)}{J}\Delta T_e - \frac{(P/2)}{J}\Delta T_L \qquad (7)$$

$$\Delta T_e = \frac{3}{2}.\frac{P}{2}.\frac{L_m}{L_r}.\left(\left[\lambda^e_{dro} \;\; -\lambda^e_{qro}\right]\begin{bmatrix}\Delta i^e_{qs}\\ \Delta i^e_{ds}\end{bmatrix} + \left[i^e_{dso} \;\; -i^e_{qso}\right]\begin{bmatrix}\Delta\lambda^e_{qr}\\ \Delta\lambda^e_{dr}\end{bmatrix}\right) \qquad (8)$$

2.3 Decoupled Control Dynamics

The IFOC dynamics for the induction machine (torque, slip angular frequency and voltage commands) can be derived from equations (1-4) respectively at $\lambda^e_{qr} = 0$ $d\lambda^e_{qr}/dt = 0$ and $\omega = \omega_e$. The torque equation and slip angular frequency for rotor field orientation are given in equations (9 and 10) while the voltage commands of the indirect field orientation controller (IFOC) are given in equations (11-14).

The block schematic of an IFOC induction machine drive system is shown in Fig. 1. It consists of a CRPWM inverter based on the space vector modulation, decoupling controller, proposed *d-q* axes stator current controllers and speed controller.

$$T_e = \frac{3}{2}.\frac{P}{2}.\frac{L_m^2}{L_r}.i^{e*}_{ds}i^{e*}_{qs} \qquad (9)$$

$$\omega_{sl} = \frac{1}{\tau_r}.\frac{i^{e*}_{qs}}{i^{e*}_{ds}} \qquad (10)$$

$$V^{e*}_{qs} - e^{e*}_{qs} = \left(L_s\sigma\frac{d}{dt}i^{e*}_{qs} + R_s i^{e*}_{qs}\right) \qquad (11)$$

$$e^{e*}_{qs} = \left(L_s\sigma + L_m^2/L_r\right)\omega_e\, .i^{e*}_{ds} \qquad (12)$$

$$V^{e*}_{ds} + e^{e*}_{ds} = \left(L_s\sigma\frac{d}{dt}i^{e*}_{ds} + R_s i^{e*}_{ds}\right) \qquad (13)$$

$$e^{e*}_{ds} = \left(L_s\sigma + L_m^2/L_r\right)\omega_e\, .i^{e*}_{qs} \qquad (14)$$

Where,

R_s : Stator resistance per phase;
R_r : Rotor resistance per phase;
L_s : Stator self inductance per phase;
L_r : Rotor self inductance per phase;
L_m : Magnetizing inductance per phase;
i^e_{ds} : Exciting current component of *d*-axis;
i^e_{qs} : Torque current component of *q*-axis;
λ^e_{dr}, λ^e_{qr} : *d*-axis and *q*-axis components of rotor flux;
e^{e*}_{ds}, e^{e*}_{ds} : *d-q*-axes components of back e.m.f;
V^{e*}_{ds}, V^{e*}_{ds} : *d-q*-axes components of the stator voltages;
τ_r : Nominal rotor time constant, $\tau_r = L_r/R_r$;
τ_s : Nominal stator time constant, $\tau_s = L_s/R_s$;
σ : Leakage flux coefficient,
$\sigma = (L_sL_r - L_m^2)/L_sL_r$;
τ'_s : Constant, $\tau'_s = \sigma\tau_s$;
τ'_r : Constant, $\tau'_r = \sigma\tau_r$;
k_{ss} : Constant, $k_{ss} = \left(1/\sigma\tau_s + 1 - \sigma/\sigma\tau_r\right)$;
K_m : Constant, $K_m = L_m/\sigma L_sL_r$;
T_e : Electromagnetic torque;
T_L : Load torque;
K_t : Torque constant, $K_t = (3P/4).(L_m^2/L_r).i^{e*}_{ds}$;
J : Motor inertia;
β : Viscous friction coefficient;
ω_r : Rotor speed;
ω : Angular frequency of the reference frame;
ω_{sl} : Slip angular frequency;
ω_n : Natural frequency;
P : Number of poles;

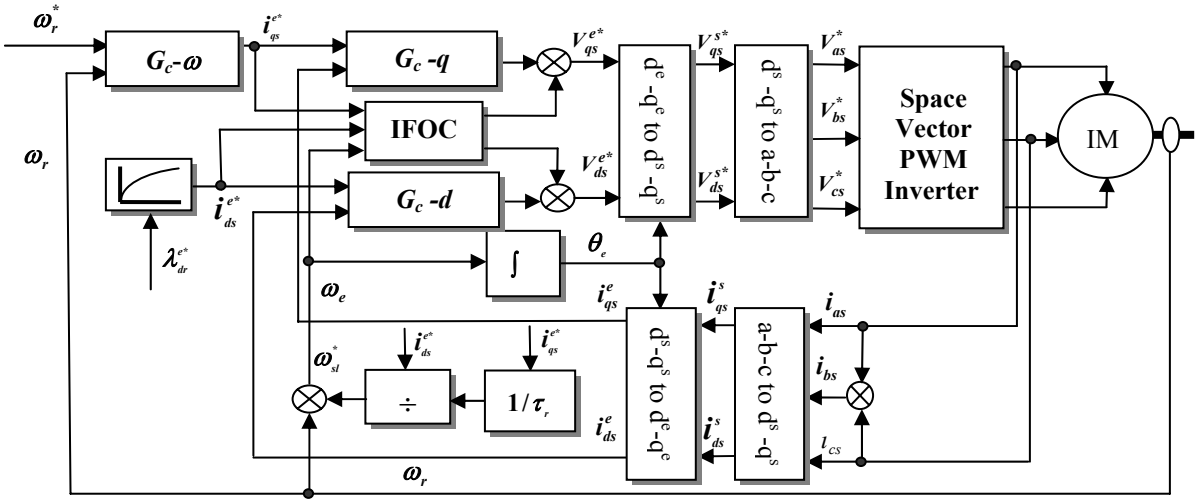

Fig. 1 Block scematic diagram of the IFOC induction motor drive system

3 Design of the Proposed 2DOF I-PD Model-Following Speed Controller

In this section, the analysis and design procedures of the 2DOF I-PD MFC speed controller is developed. The current controllers has been designed in [4] and their configuration is proportional plus integral (PI) controllers. The closed loop transfer function of the *q*-axis current loop is given by:

$$G_i(s) = \frac{K_{pq}(s + K_{PI}^i)}{\left(s^2 + \tau_i s + K_{iq}\right)} \tag{15}$$

3.1 2DOF I-PD Speed Controller

The controller consists of two parts, the I-PD controller in the feed-back loop and a feed-forward controller [15].

3.1.1 I-PD Feed-back Speed Controller

According to block diagram shown in Fig. (2), the closed loop transfer function at $T_L(s) = 0$ is given by:

$$\frac{\omega_r(s)}{\omega_{rd}(s)} = \frac{K_{tmpq}(s + K_{PI}^i)}{s^4 + \tau_{3\omega}s^3 + \tau_{2\omega}s^2 + \tau_{1\omega}s + \tau_{o\omega}} \tag{16}$$

Using the performance index ITAE robust technique, we can determine the controller parameters.

$$\frac{C(s)}{R(s)} = \frac{\omega_n^4}{s^4 + 2.1\omega_n s^3 + 3.4\omega_n^2 s^2 + 2.7\omega_n^3 s + \omega_n^4} \tag{17}$$

From equations (16) and (17), the controller parameters can derived as follows.

$$K_p^{\omega} = \frac{\left(2.7\omega_n^3 - K_{iq}/\tau_m - \omega_n^4/K_{PI}^i\right)}{K_{tmpq}K_{PI}^i} \tag{18}$$

$$K_i^{\omega} = \frac{\omega_n^4}{K_{tmpq}K_{PI}^i} \tag{19}$$

$$K_d^{\omega} = \frac{\left(2.1\omega_n - \tau_i - 1/\tau_m\right)}{K_{tmpq}} \tag{20}$$

3.1.2 I-PD Feed-forward Speed Controller

According to block diagram shown in Fig. 3, the closed loop transfer function at $T_L(s) = 0$ is given by:

$$\frac{\omega_r(s)}{\omega_{rd}(s)} = \frac{K_{tmpq}(s + K_{PI}^i)}{s^4 + \tau_{3\omega}s^3 + \tau_{2\omega}s^2 + \tau_{1\omega}s + \tau_{o\omega}}.G_{ff}(s) \tag{21}$$

Accordingly, we can obtain the feed-forward controller transfer function from equations (17 and 21) which has the following relation.

$$G_{pre}(s) = \frac{\omega_n^4}{K_{tmpq}K_i^{\omega}(s + K_{PI}^i)} \tag{22}$$

This relation is a lag compensator and to improve the relative stability of the system, we adds a lead part in this controller as follows.

$$G_{pre}^{'}(s) = \overline{K}\frac{(1+\tau_1 s)}{(1+\tau_2 s)} \tag{23}$$

3.2 Model-Following Controller (MFC)

In order to make the dynamic performance of the field oriented induction motor drive be insensitive to parameter variations and operating conditions changes, a model following controller (MFC) is designed to compensate the deviation between the desired tracking response trajectory and the actual drive system response. The closed loop tracking transfer function of the I-PD controller with the nominal model is obtained. This transfer function is used as the desired tracking characteristic of the drive system as given in equation (16). We take into consideration the current control loops. As shown in Fig. 4, a compensation control signal is obtained by the difference between the output of the MFC and the actual output of the drive system through another controller to improve the load regulation response and tracking characteristics. The compensation control signal can be obtained from a proportional (P) controller or proportional plus integral (PI) controller. The design of the MFC with P-controller and PI-controller are as follows.

3.2.1 MFC with Proportional Controller (P-MFC)

The design of the gain of the P-MFC is based on the performance index ITAE robust technique. The closed loop transfer function of the drive system taking into consideration the current control loop $G_i(s)$ is obtained from Fig. 4.

$$G_{mfc}(s) = \frac{K_{tmpq}(s + K_{PI}^i)}{s^4 + \tau_{3\omega}s^3 + \tau_{2\omega}s^2 + \tau_{1\omega}s + \tau_{o\omega}} \tag{24}$$

$$\frac{\omega_r(s)}{\omega_r^{mfc}(s)} = \frac{a_4 s^4 + a_3 s^3 + a_2 s^2 + a_1 s + a_o}{b_4 s^4 + b_3 s^3 + b_2 s^2 + b_1 s + b_o} \tag{25}$$

From equation (17 and 20), the conttrroller gain is given by:

$$K_p^{mfc} = \frac{\left(3.4\omega_n^2 - \tau_{2\omega}\right)}{K_{tmpq}K_i^{\omega}} \tag{26}$$

The stability limit of the proportional gain K_p^{mfc} of the MFC can be determined by $\omega_r^{mfc}(s) = 0$ using Routh

Hurwitz stability criterion. The selection of the limiting value of the K_p^{mfc} under parameter variation (rotor time constant and motor intertia) can be calculated from equation (27) and found from Fig. 5.

$$\omega_r^{mfc}(s) = b_4 s^4 + b_3 s^3 + b_2 s^2 + b_1 s + b_o = \begin{bmatrix} s^4 + s^3(\tau_i + 1/\tau_m + K_{tmpq} K_d^{\omega}) + s^2(\tau_{2\omega} + K_{tmpq} K_i^{\omega} K_p^{mfc}) \\ + s(\tau_{1\omega} - K_{tmpq} K_i^{\omega} + K_{tmpq} K_i^{\omega} K_{PI}^{i} K_p^{mfc} + K_{tmpq} K_i^{\omega} K_i^{\omega}) \\ + K_{tmpq} K_i^{\omega} K_i^{\omega} K_{PI}^{i} = 0 \end{bmatrix} \quad (27)$$

3.2.2 MFC with PI-Controller (PI-MFC)

Similar to P-MFC, the closed lop trnsafer function shown in Fig. 4 is given by:

$$\frac{\omega_r(s)}{\omega_r^{mfc}(s)} = \frac{c_4 s^4 + c_3 s^3 + c_2 s^2 + c_1 s + c_o}{d_4 s^4 + d_3 s^3 + d_2 s^2 + d_1 s + d_o} \quad (28)$$

From equation (17 and 22), the conttrroller gains are given by:

$$K_p^{mfc} = \frac{\left(3.4\omega_n^2 - \tau_{2\omega}\right)}{K_{tmpq} K_i^{\omega}} \quad (29)$$

$$K_i^{mfc} = \frac{\left(\omega_n^4 - K_{tmpq} K_i^{\omega} K_i^{\omega} K_{PI}^{i}\right)}{K_{tmpq} K_i^{\omega} K_{PI}^{i}} \quad (30)$$

Also, the stability limit of the MFC parameters, K_p^{mfc} and K_i^{mfc} can be obtained by $\omega_r^{mfc}(s) = 0$ using Routh Hurwitz stability criterion. The selection of the limiting value of controller gains under parameter variation (rotor time constant and motor intertia) can be calculated from equation (31) and found from Fig. 6.

$$\omega_r^{mfc}(s) = d_4 s^4 + d_3 s^3 + d_2 s^2 + d_1 s + d_o = \begin{bmatrix} s^4 + s^3(\tau_i + 1/\tau_m + K_{tmpq} K_d^{\omega}) + s^2(\tau_{2\omega} + K_{tmpq} K_i^{\omega} K_p^{mfc}) \\ + s(\tau_{1\omega} - K_{tmpq} K_i^{\omega} + K_{PI}^{i} K_p^{mfc} + K_i^{\omega} + K_i^{mfc}) \\ + K_{tmpq} K_i^{\omega} K_{PI}^{i}(K_i^{\omega} + K_i^{mfc}) = 0 \end{bmatrix} \quad (31)$$

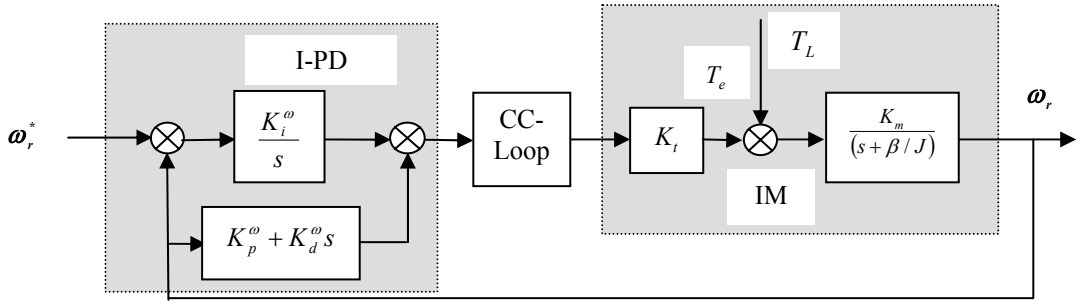

Fig. 2 Block diagram of induction machine speed control with I-PD controller

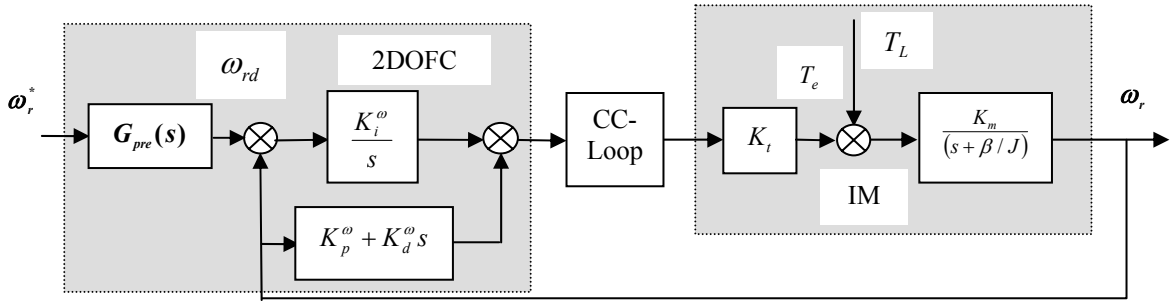

Fig. 3 The block diagram of the speed control with 2DOF I-PD controller

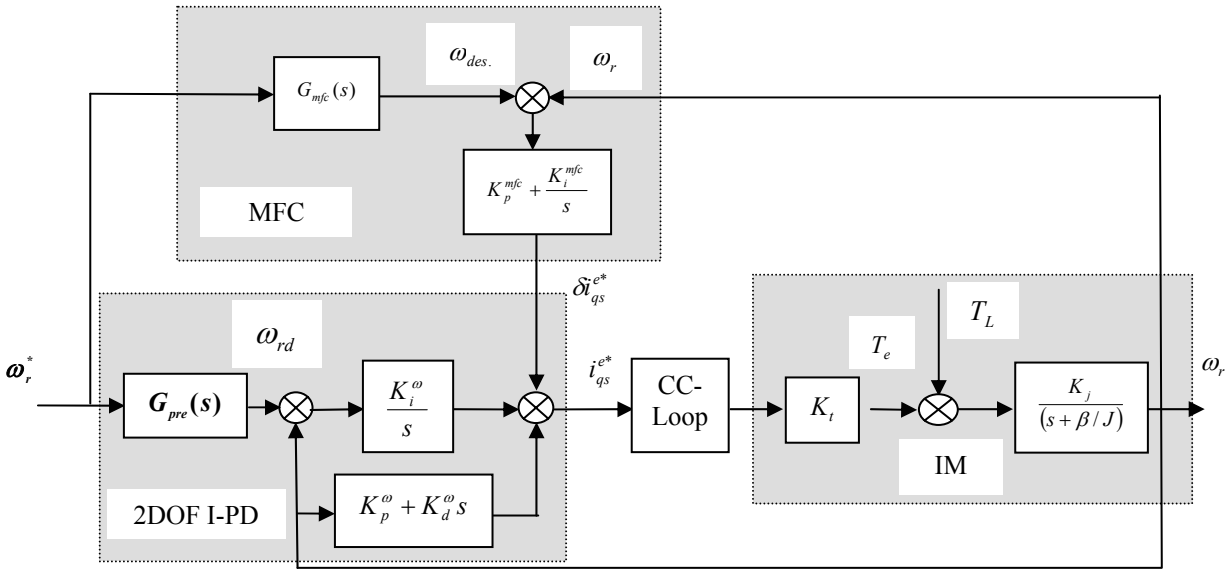

Fig. 4 The block diagram of the speed control with 2DOF I-PD model following controller

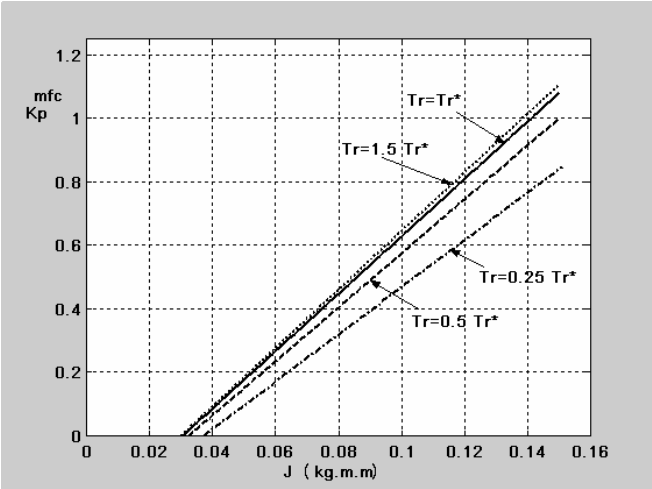

Fig. 5 The limiting values of K_p^{mfc} under parameter variations

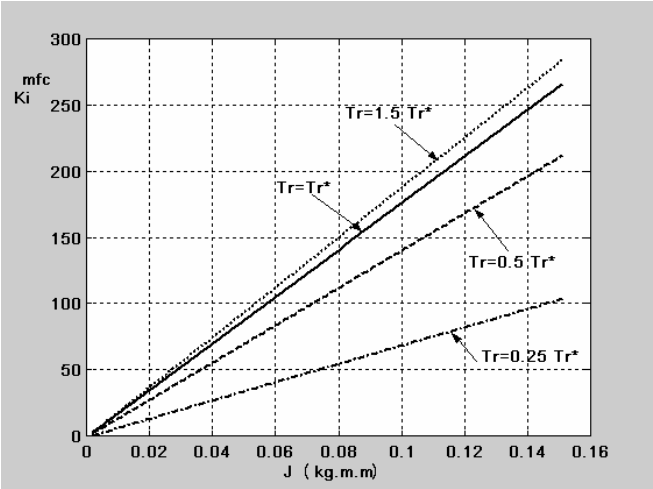

Fig. 6 The limiting values of K_i^{mfc} under parameter variations

4 Simulation Results

The simulations are carried out for the induction motor drive system with the specifications listed in Table 1.

Table 1. Machine parameters

Type: three-phase induction motor
1.5 kW, 4 poles, 380 V/3.8 A, 50 Hz
$R_s = 6.29\,\Omega, R_r = 3.59\,\Omega$, $L_s = L_r = 480\,mH, L_m = 464\,mH$,
$J = 0.038\,\text{kg.m}^2$, $\beta = 0.008345$ N.m/rad/sec

In this section, the simulations are presented to verify the feasibility of the proposed control scheme shown in Fig. 1 under the various conditions for 2DOF I-PD and 2DOF I-PD MFC speed controllers respectively. To show the validity of the the proposed control, the performance of the drive system with 2DOF I-PD MFC controller is compared with 2DOF I-PD speed controller in speed loop. The dynamic performance of the drive system for different operating conditions is studied with the application of *d-q* axes current controllers and speed controller. Taking into consideration the parameter variations of the induction machine, the performance of the drive system has been studied under load changes.

The performance of the drive system with the proposed 2DOF I-PD and 2DOF I-PD MFC speed controllers are shown in Figs. 7-13 under the conditions of external load of 11.5 N.m and the machine parameters are fixed at the nominal values.. The simulation results of the 2DOF I-PD speed controller are shown in Fig. 7 that include the

command and actual *d-q* axes currents, command torque and actual torque and the speed responses. They clearly illustrate good performance in the command tracking and the load regulation. Also, Fig. 8 shows the simulations results using 2DOF I-PD MFC speed controller. These responses obviously demonstrate the robust control performance with rapid and accurate response for the reference model. The simulation results due to step responses of the reference model and rotor speed to a step command change of rated speed are shown in Figs. 9-10 using 2DOF I-PD and 2DOF I-PD MFC speed controllers respectively. It is clearly that from Fig. 9 an obvious model-following error due to the 2DOF I-PD speed controller. With the connection of 2DOF I-PD MFC speed controller, the model-following error-driven adaptaion signal will be generated to permit a favorable model-following control performance. The rotor speed responses with the connection of the 2DOF I-PD MFC speed controller are shown in Fig. 10. Improvement of the control performance by augmenting the proposed 2DOF I-PD MFC speed controller can be observed from the results shown in Fig. 11 in command tracking and load regulation characteristics. Its clear from this Figure that the proposed 2DOF I-PD MFC speed controller provides a rapid and accurate response for the reference model within 0.5 sec. Also, the proposed controller quickly return the speed to the reference within 1.5 sec under full load with a maximum dip of 8 rad/sec. While the 2DOF I-PD speed controller gives a slow response for the reference of about 1 sec and a larg dipping in speed of about 30 rad/sec.

To investigate the effectiveness of the proposed hybrid speed controller, four cases with parameter variations in the rotor time constant, motor inertia and load torque distrubance are considered. The following possible ranges of parameter variations and external distrurbances are considered.

Case 1: $\tau_r = \tau_r^*$, J=J*, T_L=0-11.5 N.m

Case 2: τ_r=1.5 τ_r^*, J=5xJ*, T_L=0-11.5 N.m

Case 3: τ_r=0.5 τ_r^*, J=5x J*, T_L=0-11.5 N.m

Case 4: τ_r=0.25 τ_r^*, J=5x J*, T_L=0-11.5 N.m

The speed response and the load regulation performance of the drive system with the 2DOF I-PD and 2DOF I-PD MFC speed controllers are shown in Figs. (12-13) respectively under the conditions where the rotor time constant changes from $0.25\tau_r$ to $1.5\tau_r$ and the motor inertia constant changes from J to 5J. At t = 1.5 sec, external load of 11.5 N.m is applied to the drive system and removed at t=4 sec. Fig. 12 illustrates the speed tracking response and load regulation performance in the case of 2DOF I-PD speed controller with parameter variations. The speed response is significantly affected by the variations in the machine parameters. Fig. 13 shows the speed tracking response and load regulation performance in the case of 2DOF I-PD MFC speed controller under machine parameter variations. In this case, the speed response is slightly influenced by the external load than the 2DOF I-PD speed controller.

5 Conclusion

This paper proposes a robust 2DOF I-PD MFC speed controller for induction motor drive system under IFOC which guarantees the robustenss in the presence of parameter variations. Quantitative design procedures for the 2DOF I-PD and 2DOF I-PD MFC controllers have been successfully developed in this paper. First, the I-PD speed controller was designed according to the prescribed command tracking specifications and the closed loop transfer function was chosen as the reference model. Next, the feed-forward controller was designed as a lead/lag compensator to improve the disturbance rejection characteristics of the drive system. Then, a model-following controller (MFC) was designed and added to the 2DOF I-PD speed controller to preserve the good model-following characteristics under the conditions of parameter variations and external disturbance. In the design of the 2DOF I-PD MFC speed controller, the desired command-tracking specifications were defined in the reference model and the error between the outputs of the reference model and the rotor speed was used to activate the MFC controller. It follows that the rotor speed tracking response can be controlled to closely follow the response of the reference modelunder a wide range of operating conditions. The performance of the drive system and the effectiveness of the proposed controllers have been demonstrated by a wide range of simulation results. Simulation results have shown that the proposed 2DOF I-PD MFC speed controller grant accurate tracking and regulation characteristics in the face of motor parameter variations and external load disturbance. Therefore, it can be expected that the proposed control scheme can be applied to the high performance applications.

6 Appendix

$$\tau_{o\omega} = K_{tmpq} K_{PI}^{i} K_{i}^{\omega}$$

$$\tau_{1\omega} = (K_{iq} / \tau_m + K_{tmpq} K_{PI}^{i} K_{p}^{\omega} + K_{tmpq} K_{i}^{\omega})$$

$$\tau_{2\omega} = (K_{iq} + \tau_i / \tau_m + K_{tmpq} K_p^{\omega} + K_{tmpq} K_{PI}^{i} K_d^{\omega})$$

$$\tau_{3\omega} = (\tau_i + 1/\tau_m + K_{tmpq} K_d^{\omega}),\ K_{tmpq} = K_t K_m K_{pq}$$

$$K_j = (P/2)/J,\ K_{pq} = K_{qde} K_p^i,\ \tau_m = J/\beta$$

$$K_{iq} = K_{qde} K_i^i,\ \tau_{sr}^{'} = \tau_s^{'} \tau_r^{'} / (\tau_r^{'} + \tau_s^{'}(1-\sigma))$$

$$\tau_i = (1 + K_{pq} \tau_{sr}^{'}) / \tau_{sr}^{'},\ K_{qde} = 1/\sigma L_s,\ K_{PI}^i = K_i^i / K_p^i$$

$$\tau_1 > \tau_2,\ \tau_2 = (K_p^{\omega} / K_i^{\omega}),\ \overline{K} = \omega_n^4 / K_{tmpq} K_i^{\omega} K_{PI}^i$$

$$a_4 = K_i^{\omega},\ a_3 = \tau_{3\omega} K_i^{\omega},\ a_2 = K_i^{\omega}(\tau_{2\omega} + K_{tmpq} K_p^{mfc})$$

$$a_1 = K_i^{\omega}(\tau_{1\omega} + K_{tmpq} K_{PI}^i K_p^{mfc}),\ a_o = \tau_{\omega\omega} K_i^{\omega}$$

$$b_4 = 1,\ b_3 = (\tau_i + 1/\tau_m + K_{tmpq} K_d^{\omega}),\ b_2 = (\tau_{2\omega} + K_{tmpq} K_i^{\omega} K_p^{mfc})$$

$$b_1 = (\tau_{1\omega} - K_{tmpq} K_i^{\omega} + K_{tmpq} K_i^{\omega} K_{PI}^i K_p^{mfc} + K_{tmpq} K_i^{\omega} K_i^{\omega})$$

$$b_o = K_{tmpq} K_i^{\omega} K_i^{\omega} K_{PI}^i$$

$$c_4 = K_i^{\omega},\ c_3 = \tau_{3\omega} K_i^{\omega},\ c_2 = K_i^{\omega}(\tau_{2\omega} + K_{tmpq} K_p^{mfc})$$

$$c_1 = K_i^{\omega}(\tau_{1\omega} + K_{tmpq}(K_{PI}^i K_p^{mfc} + K_i^{\omega} + K_i^{mfc}))$$

$$c_o = K_i^{\omega}(\tau_{\omega\omega} + K_{PI}^i(K_i^{\omega} + K_i^{mfc}))$$

$$d_4 = 1,\ d_3 = (\tau_i + 1/\tau_m + K_{tmpq} K_d^{\omega})$$

$$d_2 = (\tau_{2\omega} + K_{tmpq} K_i^{\omega} K_p^{mfc})$$

$$d_1 = (\tau_{1\omega} - K_{tmpq} K_i^{\omega} + K_{PI}^i K_p^{mfc} + K_i^{\omega} + K_i^{mfc})$$

$$d_o = K_{tmpq} K_i^{\omega} K_{PI}^i (K_i^{\omega} + K_i^{mfc})$$

References:

[1] B. K. Bose, *Modern Power Electronics and AC Drives,* Prentice Hall, Upper Saddle River, 2002.

[2] Peter Vas, *Vector Control of AC Machines*, Oxford: Clarendon Press, 1990.

[3] Ned Mohan, *Advanced Electrric Drives: Analysis, control, and Modeling using Simulink*, MNPERE Press, USA, 2001.

[4] Fayez F. M. El-Sousy, Faeka M.H. Khater and Farouk I. Ahmed, Analysis and Design of Indirect Field Orientation Control for Induction Machine Drive System, *Proceeding of the 38th SICE annual conference, SICE99, Iwate, Japan,* July 28-30, 1999, pp. 901-908.

[5] K.B. Nordin., D.W. Novotny, and D. S.Zinger, The influence of motor parameter deviations in feedforward field orientation drive systems, *IEEE Trans. Ind. Appl.*, July/Aug., Vol. IA-21, No. 4, 1985, pp. 624-632.

[6] L. J. Garces, Parameter adaptation for the speed controlled static ac drive with a squirrel cage induction motor, *IEEE Trans. Ind. Appl., Mar./Apr.*, Vol. IA-16, No. 2, 1980, pp. 173-178.

[7] T. Matsuo T.A. and Lipo, Rotor resistance identification in the field oriented control of a squirrel cage induction motor, *IEEE Trans. Ind. Appl., May/July*, Vol. IA-21, No. 3, 1985, pp. 624-632.

[8] R. Kirshnan and F.C. Doran, Study of parameter sensitivity in high-performance inverter-fed induction motor drive system, *IEEE Trans. Ind. Appl., May/July*, Vol. IA-23, No. 4, 1992, pp. 623-635.

[9] C. M. Liaw, Design of a two-degrees-of-freedom controller for motor drives, *IEEE Trans. Automatic Control., Aug./Sept.*, Vol. AC-37, No. 4, 1992, pp. 1215-1220.

[10] C. M. Liaw and F.J. Lin, A robust speed controller for induction motor drives, *IEEE Trans. Ind. Elect., Aug./Sept*., Vol. IE-41, No. 4, 1994, pp. 308-315.

[11] Fayez F. M. El-Sousy and Maged N. F. Nashed, Robust Fuzzy Logic Current and Speed Controllers for Field-Oriented Induction Motor Drive, *The Korean Institute of Power Electronics (KIPE), Journal of Power Electronics (JPE)*, Vol. 3, No. 2, April 2003, pp. 115-123.

[12] Fayez F. M. El-Sousy and M. M. Salem, Simple Neuro-Controllers for Field Oriented Induction Motor Servo Drive System , *The Korean Institute of Power Electronics (KIPE), Journal of Power Electronics (JPE)*, Vol. 4, No. 1, January 2004, pp. 28-38.

[13] Fayez F. M. El-Sousy and M. M. Salem, High Performance Simple Position Neuro-Controller for Field-Oriented Induction Motor Servo Drives, *WSEAS Transactions on Systems, Issue 2*, Vol. 3, April 2004, pp. 941-950.

[14] Fayez F. M. El-Sousy and Maged N. F. Nashed, PID-Fuzzy Logic Position Tracking Controller for Detuned Field-Oriented Induction Motor Servo Drive, *WSEAS Transactions on Systems, Issue 2*, Vol. 3, April 2004, pp. 707-713.

[15] Fayez F. M. El-Sousy, Design and Implementation of 2DOF I-PD Controller for Indirect Field Orientation Control Induction Machine Drive System, *ISIE 2001 IEEE International Symposium on Industrial Electronics, Pusan, Korea*, June 12-16 2001, pp. 1112-1118.

[16] Matlab Simulink User Guide, The Math Work Inc., 1997

[17] C. M. Ong, *Dynamic Simulation of Electric Machinery Using Matlab and Simulink,* Printice Hall, 1998.

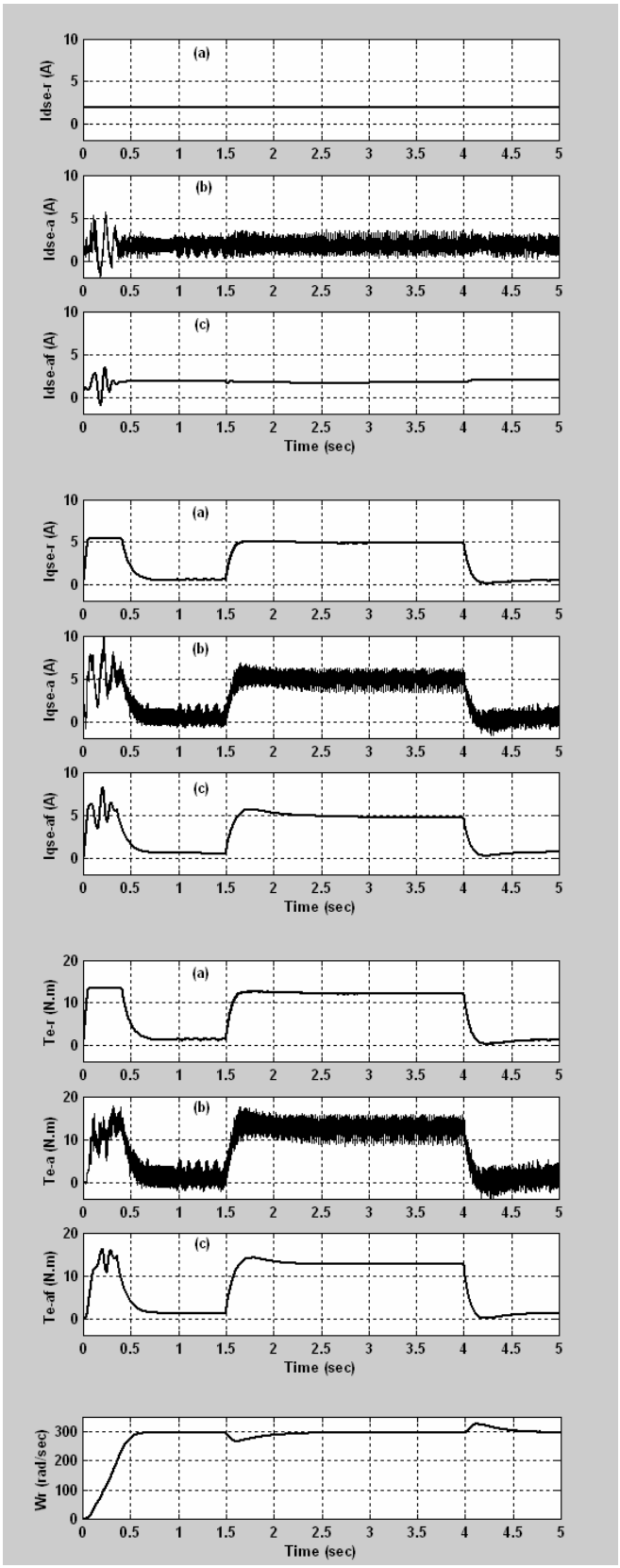

(a) Reference (b) Actual (c) Actual after filteration

Fig. 7 Step responses in speed reference and load disturbance with 2DOF I-PD speed controller

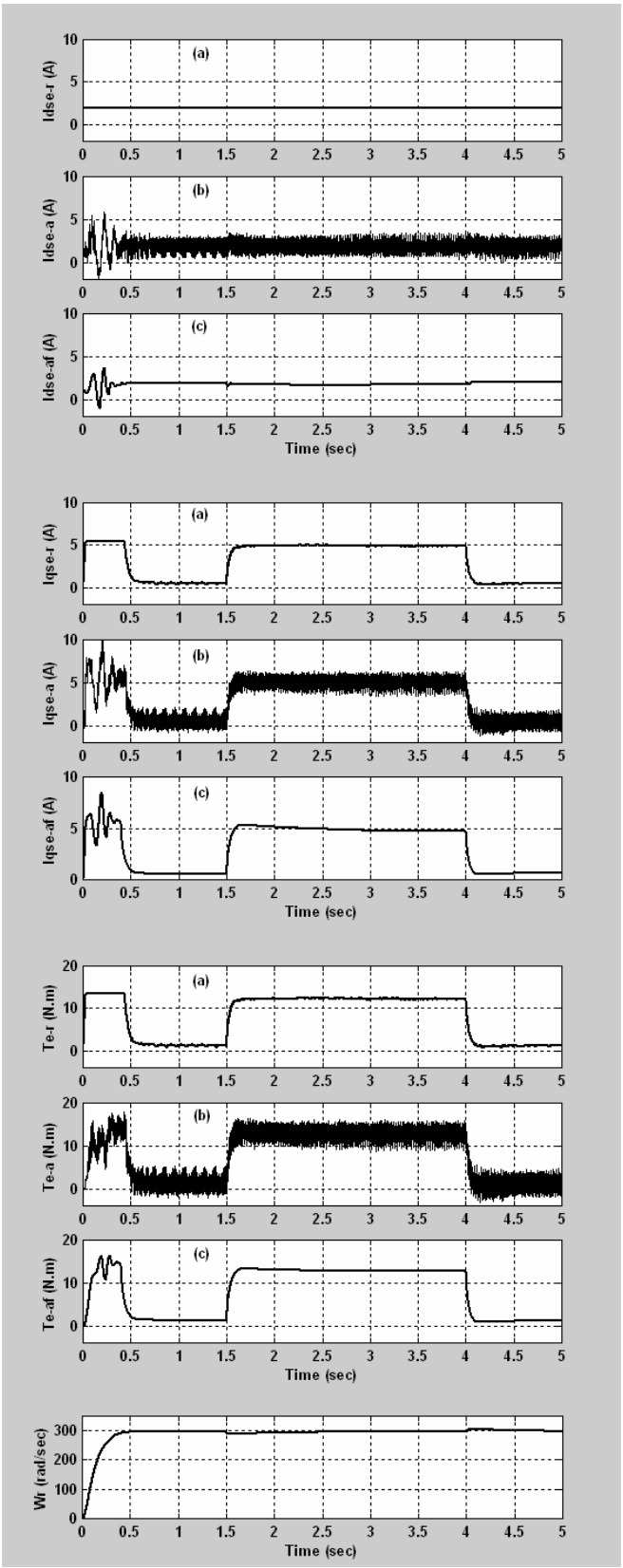

(a) Reference (b) Actual (c) Actual after filteration

Fig. 8 Step responses in speed reference and load disturbance with 2DOF I-PD MFC speed controller

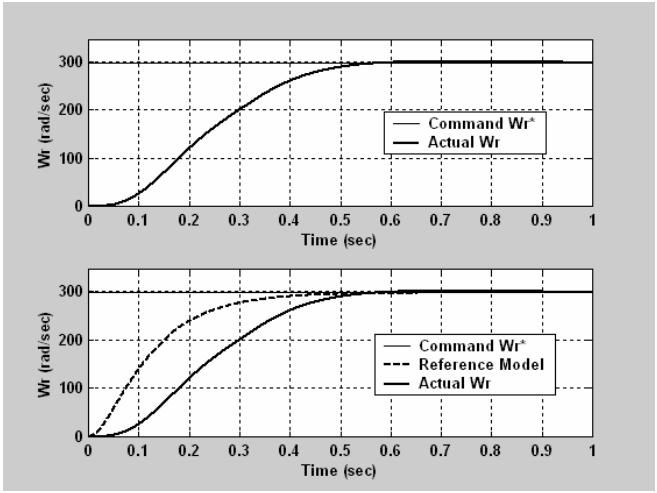

Fig. 9 The speed tracking response due step speed command change using reference model and 2DOF I-PD speed controller

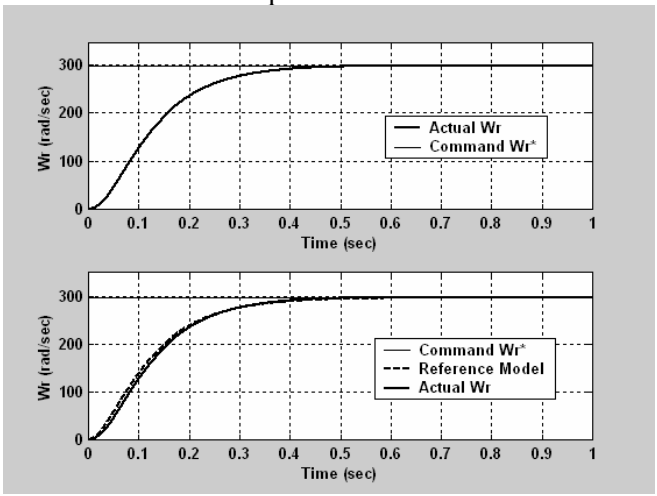

Fig. 10 The speed tracking response due step speed command change using reference model and 2DOF I-PD MFC speed controller

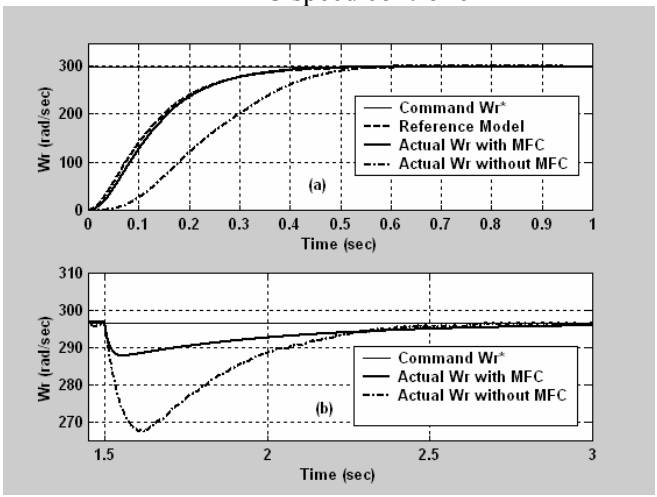

Fig. 11 Comparison between the speed tracking response and load regulation performance with and without MFC

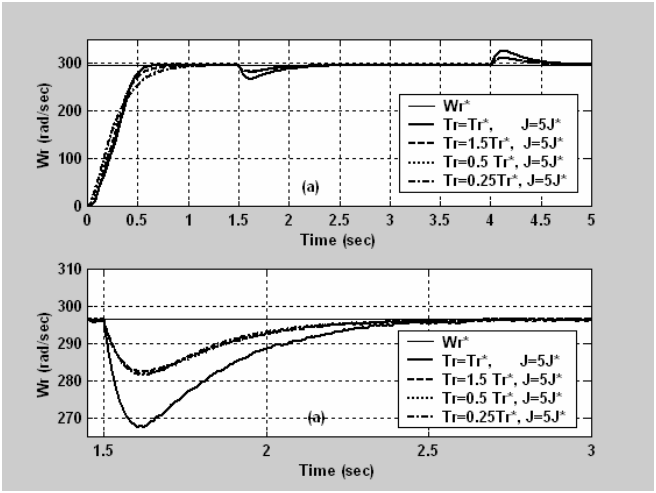

Fig. 12 The speed tracking response and load regulation performance using 2DOF I-PD speed controller under parameter variations

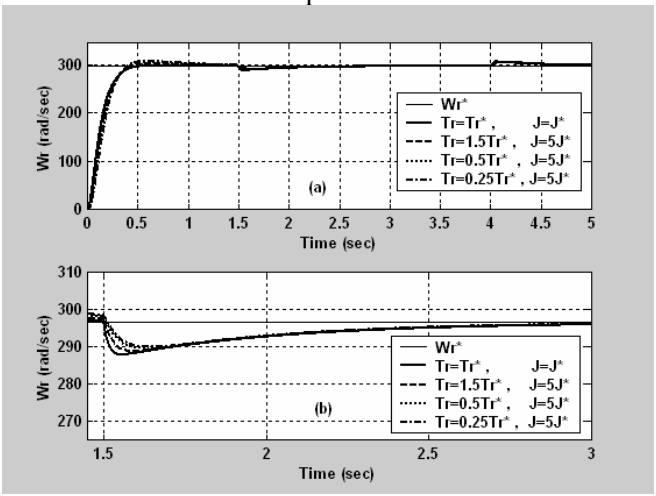

Fig. 13 The speed tracking response and load regulation performance using 2DOF I-PD MFC speed controller under parameter variations